ELSEVIER

Global and Planetary Change 9 (1994) 17–28

GLOBAL AND PLANETARY CHANGE

Surface energy balance and katabatic flow over glacier and tundra during GIMEX-91

Peter G. Duynkerke, Michiel R. van den Broeke

Utrecht University, Institute for Marine and Atmospheric Research Utrecht, Utrecht, The Netherlands

(Received September 14, 1992; revised and accepted January 14, 1993)

Abstract

The energy balance observed in the summer of 1991 during the Greenland Ice Margin EXperiment (GIMEX-91) is described. Several masts were erected along a transect perpendicular to the ice edge; from a point 90 km up the ice cap, through the ablation zone, down to a point 5.8 km within the tundra zone.

The diurnal variation of the friction velocity, sensible heat flux and latent heat flux, both on a single day (22 July) and averaged over the complete observational period are discussed. The mean daily values of the sensible heat flux (positive upwards) over the ice were negative (about -30 W/m^2), as the ice was melting during most of the observational period. On average the latent heat flux was positive, which moistened the boundary layer air flowing down the ice cap.

Up the ice cap, more than about 20 km from the ice edge, the energy balance is driven by the net radiation which causes higher fluxes during the day than during the night. The smaller (more negative) sensible heat fluxes during the night accelerate the katabatic flow; this leads to a wind maximum late at night or early in the morning. This diurnal cycle in energy balance is very similar to that observed on the slopes of Antarctica.

At the ice edge, the large difference between the radiative and thermal properties of the ice and the tundra exerts a strong thermal forcing on the katabatic flow, analogous to the land-sea breeze circulation. During day-time the thermal wind accelerates the katabatic flow, which leads to an enhancement of the turbulent exchange rate and turbulent fluxes.

1. Introduction

The Greenland Ice Margin EXperiment (GIMEX) was carried out in the Søndre Strømfjord area 67°N 50°W, in southwestern Greenland during the summers of 1990 and 1991. A major goal was to study the relation between the meteorological conditions and the mass balance of the Greenland ice sheet. In this paper we will concentrate on the determination of the turbulent fluxes, both above the ice and the tundra. The diurnal variation of the friction velocity, sensible heat flux and latent heat flux, both on a single day and averaged over the complete observational period are discussed.

In the past, only a few micro meteorological studies have been performed on the Greenland ice sheet. The most extensive ones were those made by Ambach and collaborators during the EGIG expedition of 1957 and 1966 (Ambach, 1977a,b) and the ETH-expeditions during 1991 and 1992 (Ohmura et al., 1991; Ohmura et al., 1992). The unique set up during GIMEX was that masts were erected from a point 90 km up the ice

0921-8181/94/$07.00
SSDI 0921-8181(94)E0060-C

cap, right through the melting zone, down to a point 5.8 km inside the tundra area. This set up provided us with the opportunity to study the energy balance along a transect perpendicular to the ice edge.

The large difference in the radiation and the thermal characteristics of the ice sheet and the tundra (Ohmura, 1982) has some important influences on the dynamics of the katabatic flow, especially during summer. Here, we are mainly interested in the turbulent exchange of heat and moisture between the surface and the atmosphere. We will concentrate particularly on the difference in turbulent fluxes over ice and tundra, and examine their interaction with the katabatic flow (see also Van den Broeke et al., 1993).

2. Experimental site and set up

GIMEX-91 (Greenland Ice Margin EXperiment, 1991) was carried out at 67°05′N, 50°14′W (see Fig. 1 for location of the base camp) at the boundary line between tundra and ice cap, which runs from north to south. Several meteorological masts were placed along a line perpendicular to the ice edge, from 5.8 km down the tundra to 90 km up the ice cap. In this paper we will take the x-axis from west to east and the y-axis from south to north, the origin of the co-ordinate system being the base camp. The ice front is then at about $x = 400$ m, for an overview of the experimental set up and site numbers see the bottom part of Fig. 1. The locations of the different sites are also indicated in Table 1.

In the present study measurements from seven different sites along the transect perpendicular to the ice edge were used. The most westerly site on the transect is Søndre Strømfjord weather station. The most easterly site is the boundary layer research unit of the Free University of Amsterdam. Between these two sites meteorological masts were erected by Utrecht University as indicated in Table 1. At the base camp vertical soundings were performed with a tethered balloon, up to 1000 m above ground level, sampling every 10 seconds wind speed, wind direction temperature, relative humidity and pressure. The total measuring period for the GIMEX-91 expedition was 52 days: 10 June until 31 July. We used the data for the period 10 June–31 July at site 4, 10 June–30 July at site 5, 10 June–24 July at site 6 and for the period 5 July–24 July 1991 at site 9.

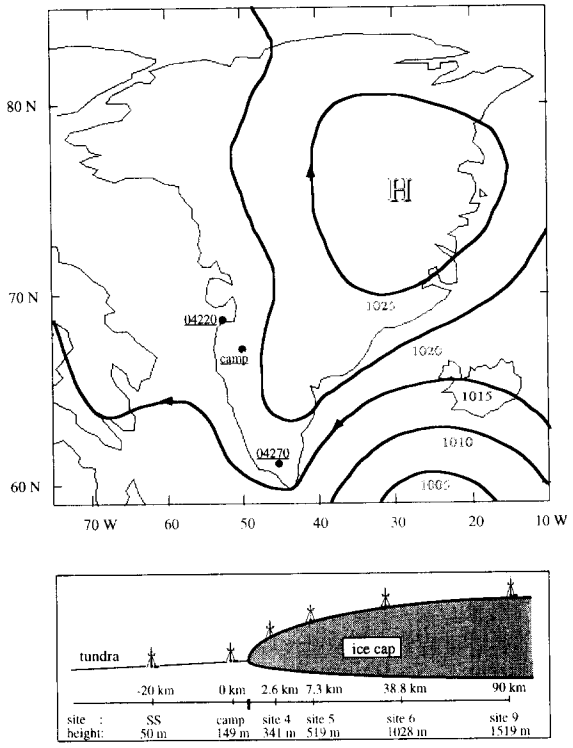

Fig. 1. Top: surface pressure map at 1200 UTC 22 July 1991.The location of the radiosonde stations Narssarssuaq (04270) and Egedesminde (04220) and the base camp are also indicated on the map. Bottom: location of the sites along the GIMEX transect, including the heights above sea level.

Table 1
The location of Søndre Strømfjord (SS) and the sites at which the masts were erected. The heights at the masts, used in this paper, at which the wind speed ($|v|$), temperature (T) and relative humidity (RH) are measured

Site	x [km]	Height [m]	$\|v\|$	T	RH
SS	-20	50	10	2	2
3	0	149			
Base camp	0	149	4.9	2, 4.9	2, 4.9
4	2.6	341	0.5, 6	0.5, 6	0.5, 6
5	7.3	519	2, 6	2, 6	
6	38.8	1028	2, 6	2, 6	
9	90.0	1519	4, 8	2, 8	2, 8

3. Determination of the fluxes

In this section a theoretical description will be given of the relations used to determine the sensible and latent heat flux in the atmospheric surface layer (section 3.1 and 3.3) and the heat flux into the soil (section 3.2).

3.1. Flux-profile relations

In the atmospheric surface layer the profiles of mean wind ($\mathbf{v} = (u, v)$), potential temperature (θ) and specific humidity (q) are related to the corresponding fluxes by the so-called flux-profile relationships:

$$\frac{\kappa z}{u_*}\left|\frac{\partial \mathbf{v}}{\partial z}\right| = \phi_m(z/L), \text{ with } u_*^2 = \left(\overline{u'w'}^2 + \overline{v'w'}^2\right)^{1/2} \quad (1.a)$$

$$\frac{\kappa z}{\theta_*}\frac{\partial \theta}{\partial z} = \phi_h(z/L), \text{ with } u_*\theta_* = -\overline{w'\theta'} \quad (1.b)$$

$$\frac{\kappa z}{q_*}\frac{\partial q}{\partial z} = \phi_h(z/L), \text{ with } u_* q_* = -\overline{w'q'} \quad (1.c)$$

$$L = \frac{u_*^2}{\kappa\{g/T_0\}(\theta_* + 0.62T_0 q_*)} \quad (1.d)$$

in which κ is the von Kármán constant, z the height above the surface, L the Monin-Obukhov length scale, g the gravitational acceleration, u_* the friction velocity, θ_* a temperature scale, q_* a humidity scale and $\phi_{m,h}$ are the dimensionless stability functions for momentum (m) and heat (h). As usual, the dimensionless stability functions for heat and moisture are taken equal.

For the dimensionless stability functions ($\zeta = z/L$) we use under unstable conditions (Dyer, 1974; Högström, 1987; Duynkerke, 1991)

$$\mu(\zeta) = (1 - \gamma_m\zeta)^{-1/4}$$
$$\phi_h(\zeta) = (1 - \gamma_h\zeta)^{-1/2} \quad (2)$$
with $\gamma_m = 20$ and $\gamma_h = 15$.

Under stable conditions there is much greater uncertainty about the functional relations (Eq. 1a–d), especially when the conditions are very stable. Duynkerke (1991) used the data of Nieuwstadt (1984) to obtain

$$\phi_m(\zeta) = 1 + \beta_m\zeta(1 + \beta_m\zeta/a)^{a-1}$$
$$\phi_h(\zeta) = 1 + \beta_h\zeta(1 + \beta_h\zeta/a)^{a-1} \quad (3)$$
with $\beta_m = 5$, $\beta_h = 7.5$ and $a = 0.8$

For $\zeta \ll 1$ the dimensionless functions (Eq. 3) are very similar to those proposed by Högström (1987), who used $\beta_m = 4.8$ and $\beta_h = 7.8$. In the surface layer the fluxes, and therefore also u_*, θ_* and q_*, are constant with height. Therefore the flux-profile relationships can be integrated analytically between two heights, i.e. z_1 and z_2 (Dyer, 1974). One can then calculate the fluxes from measurements of wind speed, temperature and specific humidity at two heights. Note that in general the wind speed, temperature and specific humidity do not have to be measured at the same heights. For instance, at the base camp we measured the wind speed at only one height (4.9 m). At this location we therefore applied the integrated flux-profile relationship for the wind between the estimated roughness length (z_0, where the wind speed is zero) and a height of 4.9 m.

3.2. Soil heat-flux

The soil heat-flux at the base camp was not measured directly. It is evaluated from the temperature measured at a depth of 2 and 5 cm in the soil. The temperature diffusion in the soil is governed by the following equation

$$\rho_s c_s \partial T_s/\partial t = \partial G(z)/\partial z \quad (4)$$

in which ρ_s is the soil density, c_s is the specific heat capacity of the soil, T_s is the temperature in the soil and $G(z)$ is the soil heat flux (positive downwards) given by

$$G(z) = \lambda_s \partial T_s/\partial z \quad (5)$$

where λ_s is the thermal conductivity of the soil. At the location where the soil temperatures are measured the soil consists mainly of a mixture of clay and sand. The area around Søndre Strømfjord is very dry, with an annual precipitation of about 250 mm. Typically, after a few days without any rainfall the soil dries out very quickly.

For sand and clay which contain very little moisture the thermal conductivity is typically 0.6–0.7 W/(m K) (Van Wijk and De Vries, 1963). With Eq.(5) and the use of the temperature measured between 2 and 5 cm depth we can calculate the soil heat-flux at the surface ($G(0)$) from

$$G(0) = 20(T_s(0.02) - T_s(0.05)) \quad (6)$$

3.3. Bowen ratio method

The sensible (H) and latent heat flux (LE) into the atmosphere cannot occur unless there is some form of energy available at the earth–atmosphere surface. The Bowen ratio method (Brutsaert, 1982) makes use of the energy budget at the surface

$$Q = H + LE + G(0) \quad (7)$$

where Q is the net radiation (positive towards the surface). From the measurements of Q and the evaluation of the soil heat flux into the soil ($G(0)$) we can calculate the sum of sensible and latent heat-flux.

In the Bowen ratio method it is assumed that the exchange coefficients for heat and moisture are the same. As a result the Bowen ratio B ($= H/LE$) can be written as $c_p \partial\theta/\partial z$ ($l_v \partial q/\partial z)^{-1}$, which we can approximate as

$$B = \frac{c_p \Delta\theta}{l_v \Delta q} \quad (8)$$

where Δ stands for the difference between the two measuring heights. We will apply this Bowen ratio method at the base camp, where we have measurements of relative humidity and temperature at 2 and 4.9 m, and compare these with fluxes obtained with the flux-profile method described in section 3.a.

4. Experimental results

The measuring period of GIMEX-91 was from 10 June to 31 July. In this chapter we will first present the synoptic situation (section 4.1) and katabatic flow at the ice masts (section 4.2) on a nearly cloud-free day. On that day, 22 July, the meteorological situation was representative for a typical summer day. In section 4.3 the energy balance over the tundra (section 4.3.1) and ice cap (section 4.3.2) will be discussed separately. In section 4.3.2 we will discuss the energy balance averaged over the complete period, and its diurnal variation. Finally in section 4.4 we will discuss the boundary layer structure at the ice edge as observed from the soundings made with the tethered balloon.

4.1. Synoptic situation

Fig. 1 shows the synoptic pressure chart at 1200 UTC 22 July 1991. Because of the low

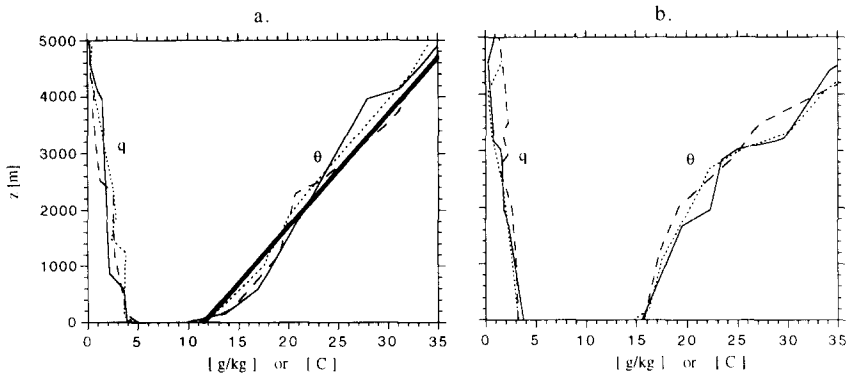

Fig. 2. Profiles of specific humidity q (g/kg) and potential temperature θ (°C) as a function of height for the radiosonde station 04220 (a) and 04270 (b): 0000 (full line), 1200 (short dashed line) and 2400 UTC (long dashed line) 22 July 1991. In (a) the thick line is a linear fit to the three observed potential temperature profiles.

density of meteorological ground and radiosonde stations over Greenland and the surrounding seas, synoptic weather systems are not well resolved in this region. On 22 July a high pressure system was centred over eastern Greenland, resulting in a southerly flow, almost parallel to the boundary line between ice and tundra at our measuring location.

Potential temperature and specific humidity profiles as a function of height from radiosonde ascents at Egedesminde (04220) and Narssarssuaq (04270) are displayed in Fig. 2a,b. The location of the two radiosonde stations is indicated in Fig. 1. The radiosonde data are not suitable for resolving the detailed boundary layer structure. However, the radiosonde data are very useful for obtaining the wind and thermodynamic structure above the boundary layer. A linear fit to the soundings at Egedesminde (04220) gives an increase in potential temperature of about 5 K/km with height, starting from a value of 284.5 K at the surface, which is shown as the thick line in Fig. 2a. Whereas the linear fit gives that the specific humidity decreases on average by about 0.9 g/(kg km), starting from a value of 4.5 g/kg at the surface.

4.2. Wind and thermodynamics at the ice masts

Let us assume a reference atmosphere for which the thermodynamic properties are only a function of height: $p_0(z)$, $\theta_0(z)$ and $q_0(z)$, in which z is the height above sea level. Moreover the reference atmosphere is motionless. In that case the two dominant mechanisms which determine the flow at the ice edge are: the diurnal variation of the temperature above the tundra and the energetics of the katabatic wind above the ice cap.

Firstly, consider the influence of the tundra on the local circulation. With a typical albedo of 0.2 for the tundra there is a large diurnal variation of the net radiation at the surface. During the summer the tundra is typically dry, which gives rise to large Bowen ratios (about 4 during day-time). The net result is that the boundary layer is strongly heated during day-time and cooled during night-time (Fig. 3a). Applying the hydrostatic equation from a certain height downwards we find that the pressure is smaller, than the reference value $p_0(z)$ in the boundary layer during day-time and larger during night-time. During day-time the pressure perturbation will be larger due to the greater depth of the boundary layer. This diurnal variation in pressure will lead to a flow analogous to the land-sea breeze circulation (Pearson et al., 1983; Ogawa et al., 1986). The flow at the ice edge will thus be accelerated during day-time and decelerated during night time.

Secondly, above the ice cap the albedo (about 0.4–0.85) is much larger than above land. Over the ice cap the diurnal variation in the net radiation is therefore much smaller. Moreover, in the ablation area melting occurs which gives rise to much smaller variations in the (surface) temperature (see for instance the temporal evolution of the temperature at the sites 4 and 5 in Fig. 3a). Higher up the ice cap the temperature will always remain below zero; as a result the diurnal variation in the temperature will be larger (Wendler et al., 1988). This increase in the diurnal variation of the temperature can already be seen at site 9 in Fig. 3a. Over the ice cap the boundary layer air is typically cooled by the transport of sensible heat towards the surface. This means that the actual temperature is lower than the reference temperature ($T_0(z)$), which causes a decrease in pressure, as a result of the sloping surface: this leads to the so-called katabatic flow. The strength of the katabatic flow is determined mainly by the inversion strength and the slope of the surface.

The boundary line between tundra and ice edge runs almost from north to south. Therefore the flow field can be assumed to be nearly two-dimensional (x,z), i.e. the gradients of all the variables with respect to y are set to zero. In that case the equations for the potential temperature (θ) and specific humidity (q) reduce to

$$\frac{\partial\theta}{\partial t} = -u\frac{\partial\theta}{\partial x} - w\frac{\partial\theta}{\partial z} - \frac{\partial\overline{w'\theta'}}{\partial z} - \frac{\partial\overline{u'\theta'}}{\partial x} - \frac{1}{\rho c_p}\frac{\partial F}{\partial z} \tag{9a}$$

$$\frac{\partial q}{\partial t} = -u\frac{\partial q}{\partial x} - w\frac{\partial q}{\partial z} - \frac{\partial\overline{w'q'}}{\partial z} - \frac{\partial\overline{u'q'}}{\partial x} \tag{9b}$$

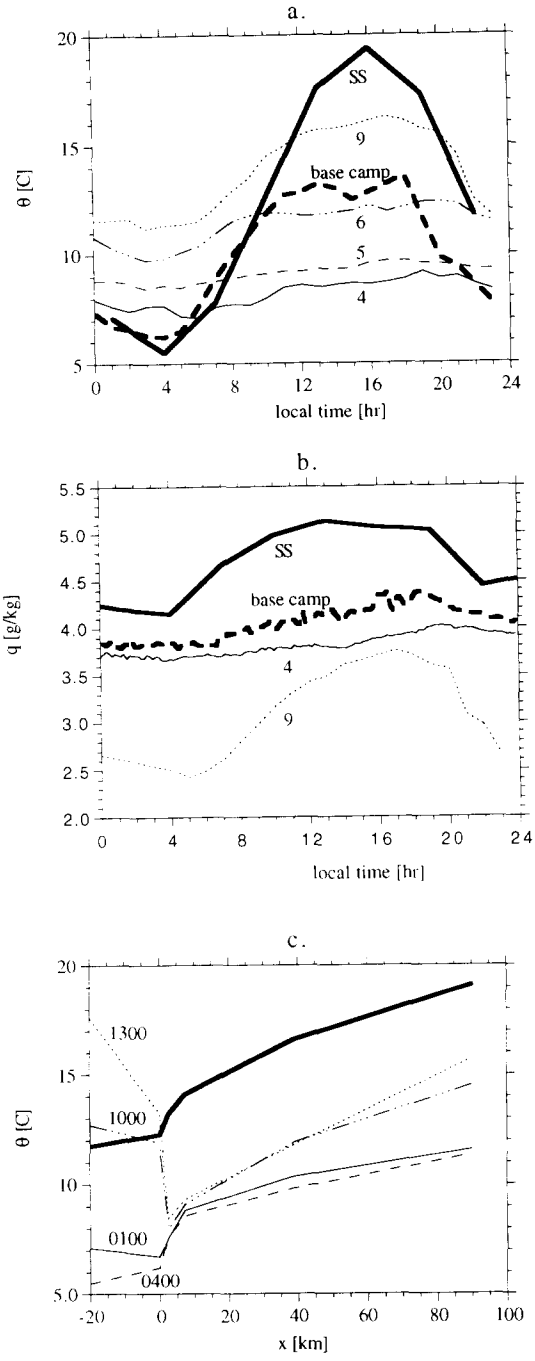

Fig. 3. The diurnal variation of the potential temperature (a) and specific humidity (b) at Søndre Strømfjord (SS) and the various sites. The potential temperature at 0100, 0400, 1000 and 1300 LT 22 July 1991 together with the observed background potential temperature at surface height (thick line) as a function of the horizontal distance is shown in (c).

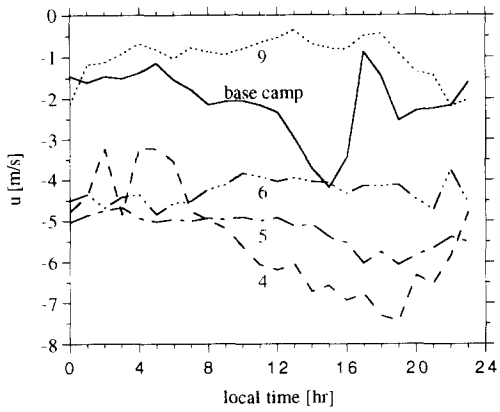

Fig. 4. The component of the wind speed perpendicular to the ice edge at the various sites for 22 July.

in which F is the net radiation (positive upwards) and the terms with the overbar represent the vertical and horizontal turbulent fluxes of heat and moisture.

$$F = F_S^{\uparrow} - F_S^{\downarrow} + F_L^{\uparrow} - F_L^{\downarrow} \tag{10}$$

where the subscripts S and L stand for shortwave and longwave, respectively. Close to the surface the vertical velocity becomes very small and as a result the vertical advection term will be small. Also the gradient of the turbulent flux in the x-direction will be rather small. Therefore the main terms in the potential temperature and specific humidity budget will be the horizontal advection term and the gradient of the turbulent transport term in the z-direction. From Fig. 3b it is clear that the specific humidity increases as the air flows down the ice cap (Fig. 4) and goes on increasing down the tundra. Apparently, evaporation takes place both above the ice cap and the tundra. Because at site 4 and the base camp there is hardly any change in the specific humidity with time there will probably be a close balance between horizontal advection and the vertical gradient of the turbulent moisture flux.

The potential temperature on the other hand decreases as the air flows down the ice cap. Which can be clearly seen from Fig. 3c where the potential temperature along the x-direction is shown at 0100, 0400, 1000 and 1300 LT. Moreover, from the linear fit in potential temperature

of the radiosonde soundings at Egedesminde (shown as thick line in Fig. 2a), a background potential temperature at surface height along the ice cap was calculated. This background potential temperature is shown as a heavy line in Fig. 3c. It is clear that the air in the katabatic layer is colder than the background potential temperature, causing the air to flow down slope. We conclude that the air above the ice cap is cooled due to turbulent mixing. At sites 4 and 5, where there is only a small diurnal variation in potential temperature in time, the horizontal advection and the vertical gradient of the turbulent heat flux are probably almost in balance.

In Fig. 4 the x-component (u) of the wind is shown as a function of time at sites 4, 5, 6, base camp and 9. The wind speed far on the ice cap (site 6 and 9) shows little diurnal variation, the highest wind speeds being recorded during the night and early morning. As the air flows down the ice cap the wind speed increases slightly, probably due to the increase in the slope of the ice cap. During day-time there is a clear increase in the u-velocity, due to the enhanced pressure gradient as a result of the heating of the tundra. At site 4 retardation of the flow is observed during night-time due to the cooling of the boundary layer over the tundra.

It is clear from the discussion above that the flow near the boundary line between tundra and ice cap is influenced by the difference in the energy balance of the tundra and the ice surface. Therefore in the following two sections we will discuss the energy balance above the ice cap (4.3.2) and tundra (4.3.1) separately.

4.3. Surface energy balance

4.3.1. Above the tundra

Over the tundra the diurnal variation in the net radiation is larger than over the ice cap, due to the smaller albedo. During the summer the tundra is relatively dry, which means that most energy is released into the atmosphere as sensible heat (typical day-time values of the Bowen ratio are about 4). The diurnal variation in the temperature above the tundra is therefore large, see for example the temperature at Søndre Strømfjord and the base camp on 22 July 1991 in Fig. 3a. At the base camp the temperature is measured at a height of 0.15, 2 and 4.9 m and the soil temperatures at a depth of 2, 5, 9.5, 18, 27 and 41 cm in the soil. For 22 July 1991 the air and some of the soil temperatures are shown in Fig. 5 as a function of time. The soil temperatures were read-out manually at selected times, represented by the symbols in Fig. 5. The soil temperature at 41 cm depth is nearly constant during the day, whereas the air temperature close to the surface undergoes a large diurnal variation. The air temperature shows that the stratification in the surface layer is stable during night-time and unstable during day-time.

From the soil temperatures measured at a depth of 2 and 5 cm we have evaluated the soil heat flux as described in section 3b. From the difference between the net radiation and soil heat flux we have evaluated, with the Bowen ratio method, the sensible (H) and latent heat flux (LE), the results of which are shown in Fig. 6a. During day-time the Bowen ratio method is fairly accurate because the soil heat flux is smaller than the net radiation. Around noon the soil heat flux becomes as large as 100 W/m^2. This makes that an error of about 50% in the soil heat flux can give an error of up to 50 W/m^2 in the sensible and latent heat flux (De Bruin and Holtslag, 1982). The sensible heat flux reaches values up to

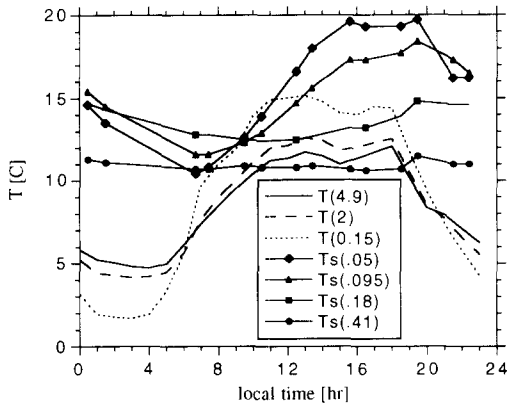

Fig. 5. The air temperature at a height of 4.9 (full line), 2 (long dashed) and 0.15 m (short dashed) and the soil temperatures (T_s) at a depth of 5 (diamonds), 9.5 (triangles), 18 (squares) and 41 cm (circles) at the base camp for 22 July.

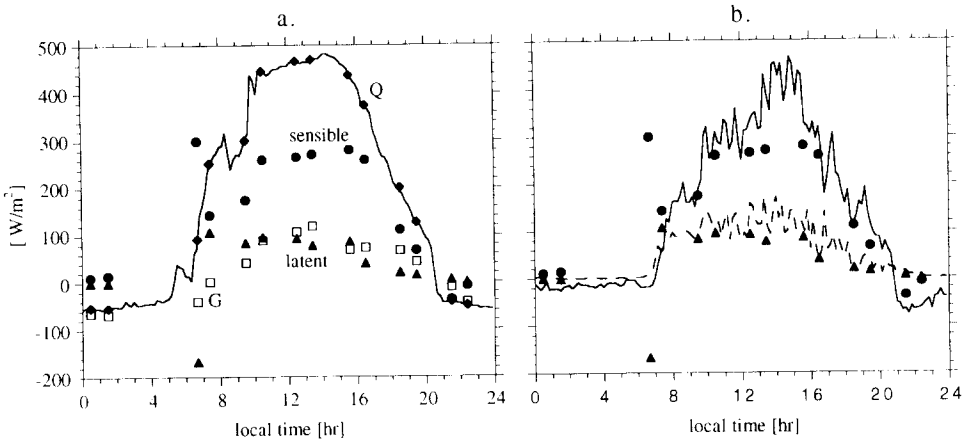

Fig. 6. (a) The diurnal variation of the measured 10-min. average (full line) and hourly average (diamonds) net radiation (Q), (squares), the soil heat flux (G) evaluated from the 2 and 5 cm soil temperature and the latent (triangles) and sensible (circles) heat flux evaluated with the Bowen ratio method for 22 July. (b) The diurnal variation of the sensible (full line) and latent (dashed line) heat flux from the profile method (full lines) and the Bowen ratio method (symbols as in a) at the base camp for 22 July.

300 W/m^2 giving rise to very strong convection over the tundra.

We have evaluated the fluxes from the profile method (section 3.1) as well. For this method the temperature and relative humidity at 2 and 4.9 m, the wind speed at 4.9 m and the roughness length for momentum (the height at which the wind speed is zero, $z_0 = 0.2$ m) are used. The sensible and latent heat flux calculated with the profile method are compared with the values from the Bowen ratio method in Fig. 6b. During daytime the profile method and Bowen ratio method yield very similar results, showing the strong convection over the tundra. The difference between both methods are quite acceptable taking into account the large terrain inhomogeneities so close to the ice edge.

4.3.2. *Above the ice*

We have calculated the friction velocity (u_*), sensible heat flux (H) and latent heat flux (LE) above the ice cap using the profile method. This method is applied at sites 4, 5, 6 and 9 using the wind speed, temperature and relative humidity measurements at the heights summarised in Table 1. The diurnal variation of the fluxes on 22 July 1991 are shown in Fig. 7. It follows that the diurnal variation on a single day is very similar to the average diurnal variation of the fluxes (Fig. 8) and the friction velocity (Fig. 9) over the complete observational period. This due to the fact that the katabatic flow is very dominantly present on the Greenland ice sheet. The average diurnal variation over the complete period has the advantage that it shows less hourly fluctuations, because as a result of the averaging these fluctuations have been smoothed out. The daily averages of the average diurnal variations are summarised in Table 2.

Far above the ice cap (site 9) the diurnal variation is mainly forced by the (local) net radia-

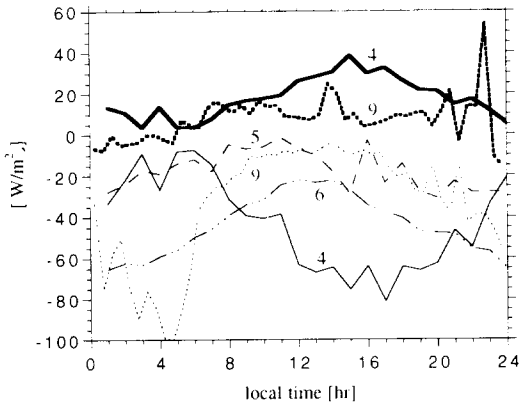

Fig. 7. The latent heat flux (thick line) and sensible heat flux (thin lines) at the various sites (numbers) as a function of local time for 22 July.

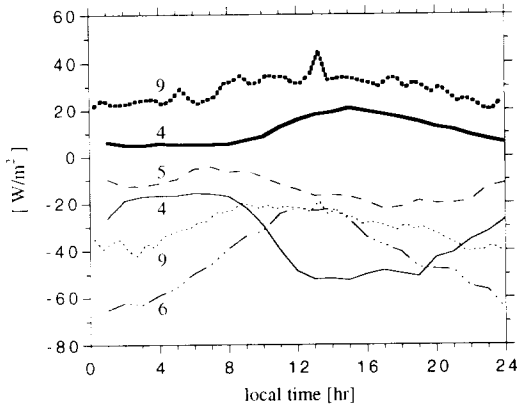

Fig. 8. The latent heat flux (thick line) and sensible heat flux (thin lines) averaged over the observational period at the various sites (numbers) as a function of local time.

tion; this leads to larger fluxes during day-time and smaller fluxes during night-time. This energy balance results in a maximum temperature during day-time and a minimum during night-time (Fig. 3a). As a result the temperature deficit of the katabatic layer, compared to that of the overlying atmosphere, is large during night-time and small during day-time. The diurnal variation in the temperature deficit results in high wind speeds during the night and low wind speeds during the day, which is reflected in the variation of the friction velocity with time. This diurnal variation in wind speed, temperature and fluxes is similar to that observed by Wendler et al. (1988) on the slopes of Antarctica.

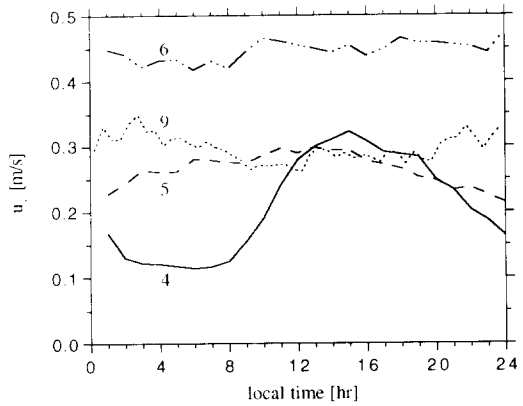

Fig. 9. The friction velocity (u_*) averaged over the observational period at the various sites above the ice as a function of local time.

Further down the ice cap, at site 6, the friction velocity (Fig. 9) is nearly independent of time, as is the wind speed. This is probably due to the thermally forced wind which the tundra imposes on the flow close to the ice edge. Due to the thermally forced wind the katabatic flow is accelerated during the day and decelerated during the night. The combined effect of the katabatic and thermal forcing is that the friction velocity is nearly independent of time. The sensible heat flux at site 6 shows nearly the same variation with time as at site 9.

Close to the ice edge, at sites 5 and 4, the thermal wind effect dominates the flow, imposing an acceleration during the day and a deceleration during the night. These effects are clearly reflected in the friction velocity observed at sites 5 and 4. The increase in the wind speed during day-time can also be seen clearly from the enhancement of the fluxes during the day.

The average fluxes over the entire period are given in Table 2. For the friction velocity, sensible heat flux and latent heat flux also the standard deviation is given in Table 2. This value is obtained by calculating first the standard deviation at a certain hour over the complete period and from these hourly values the daily average is taken. For reference also the mean energy balance at CAMP IV EGIG (Ambach, 1977a) and Carrefour station (Ambach, 1977b) are given in Tables 3 and 4, respectively. The net radiation at site 4 is 120 W/m^2, which means that about 20%

Table 2
The average friction velocity (u_*), sensible heat flux (H), latent heat flux (LE) and net radiation (Q) for the period 10 June–31 July at site 4, 10 June–30 July at site 5, 10 June–24 July at site 6, and for the period of 5 July–24 July 1991 at site 9. For the friction velocity, sensible heat flux and latent heat flux also the standard deviation is given

Site	u_* [m/s]	z_0 [cm]	H [W/m^2]	LE [W/m^2]	Q [W/m^2]
4	0.21 ± 0.10	0.08	-34 ± 19	11 ± 9	120
5	0.26 ± 0.09	0.4	-14 ± 20		
6	0.45 ± 0.13	4	-44 ± 34		
9	0.30 ± 0.14	0.8	-30 ± 20	29 ± 23	22.5

Table 3
Mean energy balance for the ablation zone at Camp IV EGIG, Greenland (69°40′05″, 49°37′58″W, 1013 m): sensible heat flux (H), latent heat flux (LS), net longwave radiation (Q_L) and net radiation (Q) in May (26–31), June, July and August (1–7) 1959 (Ambach, 1977a)

Month	H (W/m^2)	LS (W/m^{2}0	Q (W/m^2)	Q_L (W/m^2)
May	−31.2	31.5	62.6	−22
June	−26.6	19.0	75.5	−45
July	−28.9	10.0	95.9	−45
August	−30.5	30.2	52.6	−49

of the energy for melting is provided by the sensible heat flux. At site 9 all three terms, net radiation, sensible and latent heat flux, are important in the energy balance. The calculated sensible heat flux indicates that there is a transport of heat from the air in the katabatic layer towards the ice, whereas the calculated latent heat flux indicates that moisture is added to the katabatic layer as a result of evaporation. This is in agreement with the decrease in potential temperature (Fig. 3a) and increase in specific humidity (Fig. 3b) as the air flows down the ice cap.

From the wind profiles we have also calculated the roughness length for momentum. The average values [in fact ln (z_{0m})is averaged] over the whole period are given in Table 2. Going from site 9 to site 4 the surface changes from a very smooth snow/ice surface, through a hilly landscape, to ice with deep crevasses at the ice-edge. As a result one would expect an increase in roughness length from site 9 to 4. The calculations indicate

Table 4
Mean energy balance for Carrefour station, Greenland (69°49′25″N, 47°25′57″W, 1850 m): sensible heat flux (H), latent heat flux (LS), net longwave radiation (Q_L) and net radiation (Q) in May (20–31), June and July (1–28) 1967 (Ambach, 1977b)

Month	u_* (m/s)	H (W/m^2)	LS (W/m^2)	Q (W/m^2)	Q_L (W/m^2)
May	0.28	−18.1	10.6	−3.4	−59
June	0.26	−13.1	12.0	6.5	−40
July	0.29	−15.9	13.7	11.3	−46

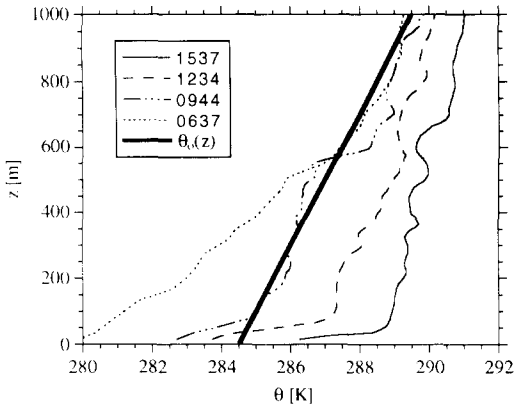

Fig. 10. The potential temperature as a function of height at the base camp at 0637, 0944, 1234 and 1537 LT 22 July 1991. The thick line is the linear fit to the radiosonde profiles at Egedesminde (discussed in section 4.a) which is also shown in Fig. 2a.

a roughness length in the range of several centimetres to less than one millimetre.

4.4. Boundary layer structure at the ice edge

The tethered balloon data were taken up to a height of about 1000 m at the base camp. Fig. 10 shows the potential temperature. The potential temperature reveals a very stable lapse rate in the lower 100 m, whereas above 100 m the lapse rate becomes less stable. The potential temperature at screen level at Søndre Strømfjord reaches a maximum of 292.5 K during the day. Therefore above the tundra a convective boundary layer develops, having a height of about 1500 m. The stable lapse rate in the lower 100 m of the tethered balloon data is due to the katabatic flow down the ice cap. This air is typically cold and is heated as the air flows over the tundra. This can be seen from the heat fluxes at the base camp which show a very unstable potential temperature profile in the lower metres of the atmosphere. The balloon data show a very stable layer from 15 m upwards, which indicates that this unstable layer is still very shallow and that the katabatic flow at the balloon site is therefore hardly influenced by the tundra.

5. Conclusions

During summer, in the melting zone of the Greenland ice sheet, the boundary layer is usually stably stratified. Interesting aspects of this stably stratified boundary layer are the horizontal homogeneity and the moderate to high wind speeds. The latter means that the turbulent exchange rates are relatively large for a stable boundary layer.

In the melting zone of the ice sheet a downward sensible heat flux of approximately 32 W/m^2 is observed, which compares favourably with the data collected at Camp IV EGIG (Ambach, 1977a), at an altitude of 1013 m, presented in Table 3. The latent heat flux (Table 2) and specific humidity (Fig. 3b) show that evaporation takes place throughout the melting zone. Moreover, the values of the latent heat flux indicate that evaporation increases higher up the ice cap up to the equilibrium line.

At the ice edge (site 4) the sensible heat flux makes up about 20% of the total energy available for melting the ice, 80% is provided by the net radiation. At site 9, 90 km up the ice cap, all three terms: sensible heat flux, latent heat flux and net radiation are important in the energy balance.

At site 9 the diurnal variation in wind speed, temperature and fluxes is similar to that observed on the slopes of Antarctica (Wendler et al., 1988). The energy balance is driven by the net radiation which causes higher fluxes during day-time than during night-time (Fig. 8). At the ice edge (sites 4 and 5) the katabatic flow is modified by the thermal wind effect induced by the tundra (Van den Broeke et al., 1994). The combined effect of the katabatic and thermal forcing is that the turbulent exchange is enhanced during the day.

In summary, the large difference between the radiative and thermal characteristics of the tundra and the adjacent ice leads to a large difference in energy balance. During summer, this creates a strong thermally forced wind at the ice edge, which modifies the regular katabatic flow. The flow induced by this thermal forcing, significantly influences the diurnal variation of the energy balance over a strip about 20 km wide along the ice edge. Further research needs to be done to find out how this thermal forcing affects the local circulation.

6. Acknowledgements

Our thanks go to the members of the GIMEX teams, without whose help these measurements could never have been made. Generous logistic support was provided by the staff of the Weather Service in Søndre Strømfjord. The observations from site 9 were kindly supplied by Hans Vugts and Edwin Henneken from the Free University of Amsterdam.

Financial support for this work was obtained from the Dutch National Research Programme on Global Air Pollution and Climate Change (contract 276/91-NOP), from the Commission of the European Communities (contract EPOC-CT90-0015), and from the Netherlands Organisation for Scientific Research (Werkgemeenschap CO_2-Problematiek).

7. References

Ambach, W., 1977a. Untersuchungen zum Energieumsatz in der Ablationszone des Grönländischen Inlandeises: Nachtrag. In: Expedition Glaciologique Internationale au Groenland, 4, No. 5. Bianco Lunos, København, pp. 63.

Ambach, W., 1977b. Untersuchungen zum Energieumsatz in der Akkumulationszone des Grönländischen Inlandeises: Nachtrag. In: Expedition Glaciologique Internationale au Groenland, 4, No. 7, Bianco Lunos, København, pp. 44.

Brutsaert, W., 1982. Evaporation into the Atmosphere. Reidel, Dordrecht, 299 pp.

De Bruin, H.A.R. and Holtslag, A.A.M., 1982. A simple parameterization of the surface fluxes of sensible and latent heat during daytime compared with the Penman–Monteith concept. J. Appl. Meteorol., 21: 1610–1621.

Duynkerke, P.G., 1991. Radiation fog: a comparison of model simulation with detailed observations. Mon. Weather Rev., 119: 324–341.

Dyer, A.J., 1974. A review of flux-profile relationships. Boundary-Layer Meteorol., 7: 363–372.

Högström, U., 1987. Non-dimensional wind and temperature profiles in the atmospheric surface layer: A re-evaluation. Boundary-Layer Meteorol., 42: 55–78.

Ogawa, Y., Ohara, T., Wakamatsu, S., Diosey, P.G. and Uno, I., 1986. Observation of lake breeze penetration and subsequent development of the thermal internal boundary

layer for the Nanticoke II shoreline diffusion experiment. Boundary-Layer Meteorol., 35: 207–230.

Ohmura, A., 1982. Climate and energy balance on the Arctic tundra. J. Climatol., 2: 65–84.

Ohmura, A. et al., 1991. Energy and mass balance during the melt season at the equilibrium line altitude, Paaktisoq, Greenland Ice Sheet. ETH Greenland Exped. Progr. Rep., 1, Dep. Geogr. ETH, Zürich, 108 pp.

Ohmura, A. et al., 1992. Energy and mass balance during the melt season at the equilibrium line altitude, Paaktisoq, Greenland Ice Sheet. ETH Greenland Exped. Progr. Rep., 2, Dep. Geogr. ETH, Zürich, 94 pp.

Nieuwstadt, F.T.M., 1984. The turbulent structure of the stable, nocturnal boundary layer. J. Atmos. Sci., 41: 2202–2216.

Pearson, R.A., Carboni, G. and Brusasca, G., 1983. The sea breeze with mean flow. Q.J. R. Meteorol. Soc., 109: 809–830.

Van den Broeke, M.R., Duynkerke, P.G. and Oerlemans, J., 1994. The observed katabatic flow at the edge of the Greenland ice sheet during GIMEX-91. Global Planet. Change, 9: 3–15.

Van Wijk, W.R. and De Vries, D.A., 1963. Periodic temperature variations in a homogeneous soil. In: W.R. Van Wijk (Editor), Physics of Plant Environment. North Holland, Amsterdam, pp. 102–143.

Wendler, G., Ishikawa, N. and Kodamo, Y., 1988. The heat balance of the icy slope of Adélie land, eastern Antarctica. J. Appl. Meteorol., 27: 52–65.